

**Electronic Supplementary Information**

**Ms. ID: LC-ART-06-2012-040660**

**1 August, 2012**

**Dual-Channel Bipolar Electrode Focusing: Simultaneous Separation  
and Enrichment of Both Anions and Cations**

Kyle N. Knust, Eoin Sheridan, Robbyn K. Anand, and Richard M.  
Crooks

Department of Chemistry and Biochemistry, Center for  
Electrochemistry, and the Center for Nano- and Molecular Science  
and Technology, The University of Texas at Austin, 1 University  
Station, A5300, Austin, Texas 78712-0165, U.S.A.

13 pages

**Dual-channel focusing with TrisH<sup>+</sup> buffer in the top and bottom**

**channels**. To show that a steep electric field gradient forms in the bottom channel only in the presence of buffer capable of being neutralized by electrogenerated H<sup>+</sup>, we performed the following control experiments. For all experiments within this subsection, the top and bottom channels were filled with 40 mM TrisH<sup>+</sup> buffer (pH 8.1) containing 1.0 μM BODIPY<sup>2-</sup>. All dual-channel experiments were carried out with V<sub>1</sub> at 30.0 V, and V<sub>2</sub>, V<sub>3</sub>, and V<sub>4</sub> grounded (Scheme 2a, main text).

Similar to the result in the main text with acetate buffer in the bottom channel, now with TrisH<sup>+</sup> buffer in the bottom channel, the red trace of Figure S-1a shows the 30.0 V potential difference between reservoirs V<sub>1</sub> and V<sub>2</sub> in the top channel deviates from linearity as a result of water reduction and corresponding neutralization of TrisH<sup>+</sup> (eqs 2 and 3, main text, respectively). This creates an ion depletion zone and causes the formation of a subsequent electric field gradient (Figure S-1a black trace). Analyte enriches along the electric field gradient via the CFGF mechanism. Accordingly, an enriched band of the anionic tracer, BODIPY<sup>2-</sup>, is observed in Figure S-1b (top image) with an EF of 767-fold (1.6-fold/s).

Although enrichment in the top channel is not greatly influenced by the composition in the bottom channel, enrichment in the bottom channel is a strong function of its solution

composition. For example, we showed that acetate buffer in the bottom channel results in a steep electric field gradient (Figure 1e, black trace, main text) due to buffer neutralization. However, when the bottom channel is filled with  $\text{TrisH}^+$  buffer, a shallow electric field gradient (Figure S-1c, black trace) results that is unable to support a significant degree of enrichment. Similar to Figure 1d (bottom image) in the main text,  $\text{BODIPY}^{2-}$  accumulates adjacent to the BPE (Figure S-1b, bottom image). The EF in the bottom channel is lower (58-fold, 0.2-fold/s) than in the top channel as a consequence of the shallow electric field gradient and lack of convective flow.

We attempted to generate a compact enriched band of  $\text{BODIPY}^{2-}$  in the bottom channel by introducing PDF, but this was unsuccessful. This is because the faradaic reaction at the BPE anode results in formation of  $\text{H}^+$  (eq 1, main text); hence, there is no neutralization of  $\text{TrisH}^+$  buffer and no depletion region forms. The key point is that with  $\text{TrisH}^+$  buffer present in both the top and bottom channels, an ion depletion zone forms in the top channel which supports enrichment, while in the bottom channel, the absence of an ion depletion zone prevents enrichment.

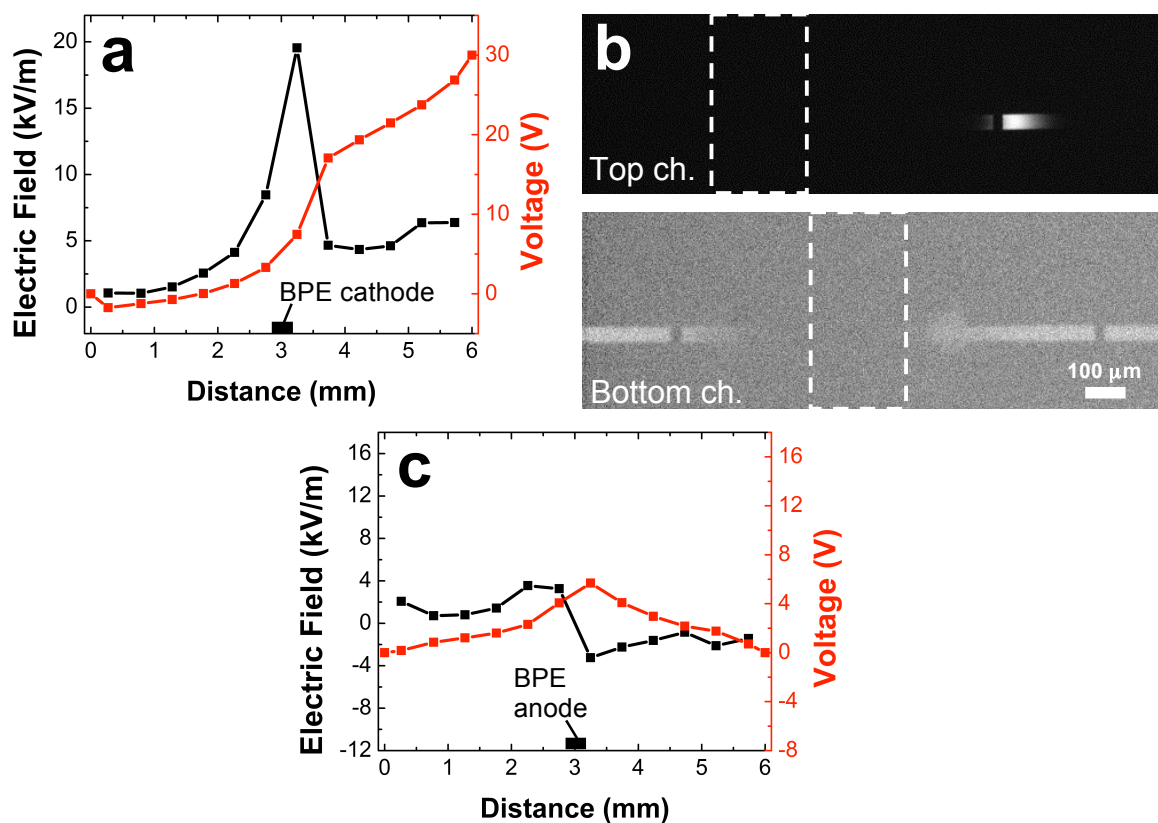
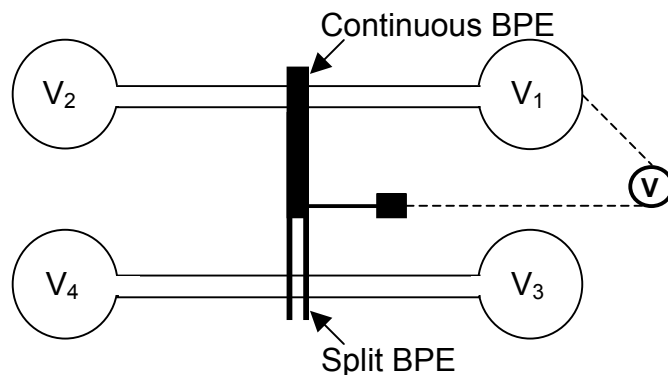


**Figure S-1.** (a) Plot of the axial electric field (black trace) and voltage drop (red trace) in the top channel. (b) Fluorescence micrographs of enriched BODIPY<sup>2-</sup> bands in the top and bottom channels. The location of the BPE is indicated by dashed white lines. (c) Plot of the axial electric field (black trace) and voltage drop (red trace) in the bottom channel. The top and bottom channels were filled with 40 mM TrisH<sup>+</sup> buffer (pH 8.1) containing 1.0 μM BODIPY<sup>2-</sup>.  $V_1 = 30.0$  V and  $V_2$ ,  $V_3$ , and  $V_4$  were grounded.

**Measurement of  $E_{elec}$ .** For all measurements of the BPE floating potential, the microchannels were initially filled with either 40 mM TrisH<sup>+</sup> buffer (pH 8.1) or 40 mM acetate buffer (pH 4.8) and rinsed by applying 10.0 V to  $V_1$  and  $V_3$ , while grounding  $V_2$  and  $V_4$  (Scheme 2a, main text). This voltage was applied for 5 min to allow electroosmosis to rinse the channel. Because EOF is somewhat suppressed at pH 4.8, pressure driven flow (PDF) was also used to rinse the channel.<sup>1</sup> Next, the rinse buffer was removed from each reservoir and replaced with 60.0  $\mu$ L of 40 mM buffer containing 1.0  $\mu$ M BODIPY<sup>2-</sup>, 10.0  $\mu$ M Ru(bpy)<sub>3</sub><sup>2+</sup>, or a mixture of 1.0  $\mu$ M BODIPY<sup>2-</sup> and 10.0  $\mu$ M Ru(bpy)<sub>3</sub><sup>2+</sup>.

The device design used to measure the floating potential of the BPE is depicted in Scheme S-1 (not to scale). A Au BPE with a continuous and split pole was used to bring two PDMS microchannels (6 mm long, 50  $\mu$ m wide, and 8.7  $\mu$ m high) into electrical contact.<sup>2</sup> A Au contact pad extending from the BPE was used to make a connection between the BPE, a hand-held voltmeter ("V" in Scheme S-1), and the coiled Au driving electrode in reservoir  $V_1$ . A 30.0 V potential was applied to  $V_1$  with respect to the grounded  $V_2$ ,  $V_3$ , and  $V_4$  reservoirs. The potential difference between the BPE and  $V_1$  was recorded on a personal computer using PC-Link software (Sinometer Instruments, ShenZhen, China).



### Scheme S-1

Figure S-2a shows a representative measurement of  $E_{\text{elec}}$  before, during, and after 30.0 V was applied to V<sub>1</sub>. During this experiment, both the top and bottom channels were filled with 40 mM TrisH<sup>+</sup> buffer. At  $t = 0$ ,  $E_{\text{elec}} = 0$ , but at later times (29 s - 227 s) it achieved a value of ~6 V before dropping again to 0 V at 228 s when the power source was turned off. The key finding is that  $E_{\text{elec}}$  attains a relatively constant value throughout the entire experiment. In Figure S-2b, with the top channel filled with 40 mM TrisH<sup>+</sup> buffer and the bottom channel filled with 40 mM acetate buffer, the voltage of the BPE floats to a higher value of  $E_{\text{elec}}$  (~15 V). This result is due to a depletion region forming adjacent the BPE anode when acetate buffer is neutralized in the bottom channel by electrogenerated H<sup>+</sup>.

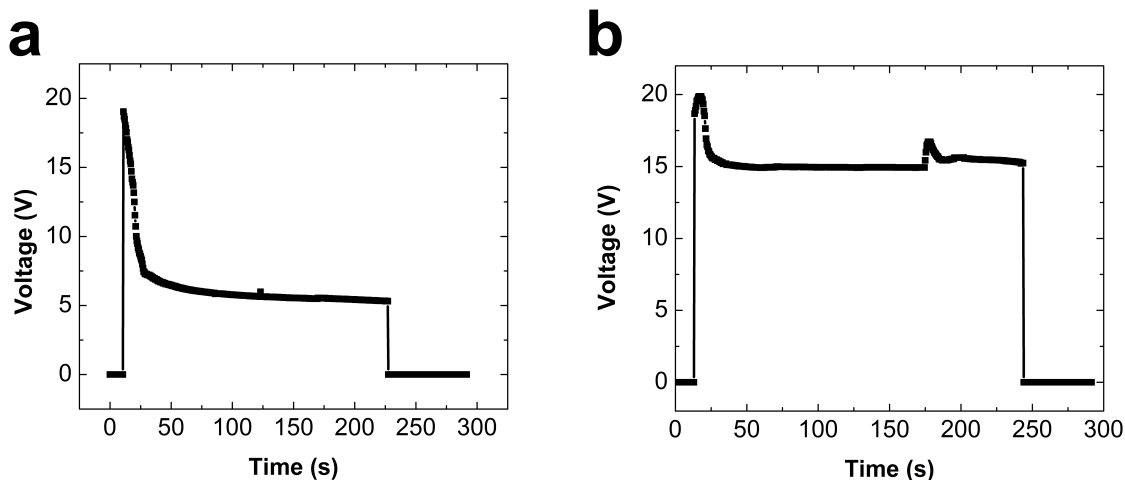
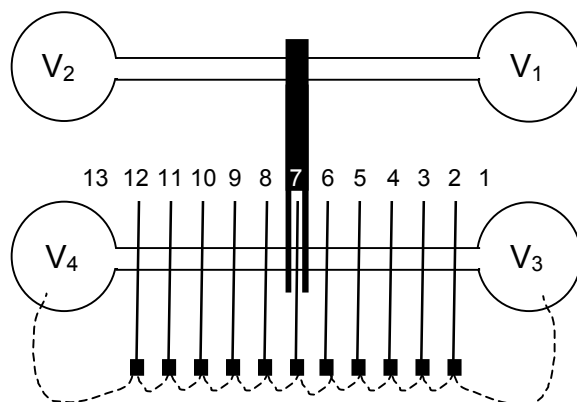


**Figure S-2.** (a) Plot of the floating BPE voltage vs. time with both the top and bottom channels filled with 40 mM TrisH<sup>+</sup> buffer. (b) Plot of the floating BPE voltage vs. time with the top channel filled with 40 mM TrisH<sup>+</sup> buffer and the bottom channel filled with 40 mM acetate buffer. During each of these experiments, 30.0 V was applied to V<sub>1</sub>, while V<sub>2</sub>, V<sub>3</sub>, and V<sub>4</sub> were grounded.

**Explanation of the positive and negative electric field in the bottom channel.** All axial electric field measurements in the bottom channel were performed with the device depicted in Scheme S-2 (not to scale). A Au BPE having a continuous and split pole was used to bring two PDMS microchannels (6 mm long, 50 μm wide, and 8.7 μm high) into electrical contact. Eleven 50 μm-wide Au microbands were spaced 495 μm apart (center-to-center) to measure the axial electric field. The two distal electric field measurements were made versus the coiled Au electrodes placed in

the reservoirs. As depicted in Scheme S-2, microband number 7 was centered between the split portion of the BPE with the remaining microbands spaced evenly toward the reservoirs.



#### Scheme S-2

The microbands extended from below the PDMS monolith to expose a contact pad allowing connection to a breakout board and scanning digital multimeter (SDMM, Model 2700, Keithley Instruments, Cleveland, OH). The procedure for making these measurements has been previously reported.<sup>3,4</sup> After preparing the device as described in the Experimental Section of the main text, the SDMM was turned on and began collecting potential difference measurements between driving electrode 1 and microband 2 (Scheme S-2). Next, the potential difference between microbands 2 and 3 was measured. The SDMM continued to sequentially measure the potential difference between each set of microbands until a measurement between microband 12 and driving electrode 13 was completed (Scheme S-2). The acquisition time for each voltage measurement was  $\sim 0.1$  s, and the voltage



between pairs of microbands was recorded every 2.0 s. After ~5 measurements of the axial electric field across the entire microchannel with no voltage applied, 30.0 V was applied to  $V_1$ , with  $V_2$ ,  $V_3$ , and  $V_4$  grounded. Now, under enrichment conditions, the SDMM continued to collect electric field data for the remainder of each experiment. Figure 1e (black trace, main text) shows a representative axial electric field measurement made across the entire length of the microchannel (6 mm to 0 mm).

When collecting measurements from 1 to 13 (Scheme S-2), the electric field in the region from 1-7 is negative. Because voltage in the bottom channel is highest at the channel center (Figure 1e, main text) and drops to 0 V at the grounded reservoirs, voltage at the first microband measured is lower than the voltage at the second microband. This means the difference between these measurements is negative, hence resulting in a negative electric field. Conversely, in the region from 7-13, the electric field is positive because the voltage at the first microband measured is higher than the voltage at the second microband. If the axial electric field were measured from 13 to 1 (Scheme S-2), rather than from 1 to 13, the opposite regions would have positive or negative electric fields.

**Simultaneous separation and enrichment of anions and cations in the top channel.** Devices for this subsection were prepared as described in the Experimental Section of the main text. The top channel was filled with a solution of 1.0  $\mu\text{M}$  BODIPY<sup>2-</sup>, 10.0  $\mu\text{M}$  Ru(bpy)<sub>3</sub><sup>2+</sup>, and 40 mM TrisH<sup>+</sup> buffer (pH 8.1). The bottom channel was filled with a solution of 1.0  $\mu\text{M}$  BODIPY<sup>2-</sup>, 10.0  $\mu\text{M}$  Ru(bpy)<sub>3</sub><sup>2+</sup>, and 40 mM acetate buffer (pH 4.8). With  $V_1$  and  $V_2$  at 30.0 V and  $V_3$  and  $V_4$  grounded (Scheme 2a, main text), BODIPY<sup>2-</sup> and Ru(bpy)<sub>3</sub><sup>2+</sup> were seen to simultaneously separate and enrich in the bottom channel with the addition of PDF from left to right. Simultaneous separation and enrichment was also observed in the top channel with PDF from right to left.

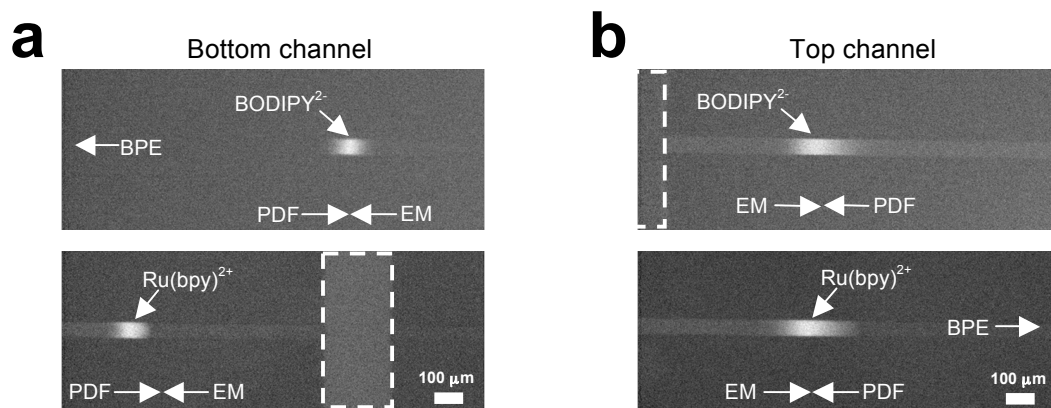


**Figure S-3.** (a) Fluorescence micrographs of enriched bands of BODIPY<sup>2-</sup> and Ru(bpy)<sub>3</sub><sup>2+</sup> in the bottom channel with PDF from left to right. The location of the BPE is indicated by dashed white lines or an arrow. (b) Fluorescence micrographs of enriched bands of BODIPY<sup>2-</sup> and Ru(bpy)<sub>3</sub><sup>2+</sup> in the top channel with PDF from

right to left. The solution composition in the top channel was 1.0  $\mu\text{M}$  BODIPY<sup>2-</sup>, 10.0  $\mu\text{M}$  Ru(bpy)<sub>3</sub><sup>2+</sup>, and 40 mM TrisH<sup>+</sup> (pH 8.1) with the bottom channel composed of 1.0  $\mu\text{M}$  BODIPY<sup>2-</sup>, 10.0  $\mu\text{M}$  Ru(bpy)<sub>3</sub><sup>2+</sup>, and 40 mM acetate (pH 4.8).  $V_1, V_2 = 30.0$  V and  $V_3, V_4$  were grounded.

Figure S-3a shows that in the bottom channel BODIPY<sup>2-</sup> enriches to the right of the BPE anode (indicated by white dashed lines or an arrow), while Ru(bpy)<sub>3</sub><sup>2+</sup> enriches to its left with PDF from left to right. Roughly 15 seconds after Figure S-3a was collected, two additional fluorescence micrographs (Figure S-3b) were recorded showing that in the top channel BODIPY<sup>2-</sup> enriches to the right of the BPE cathode (indicated by white dashed lines or an arrow), while Ru(bpy)<sub>3</sub><sup>2+</sup> enriches to its left with PDF from right to left. These results qualitatively demonstrate that with  $V_1$  and  $V_2$  at 30.0 V and  $V_3$  and  $V_4$  grounded (Scheme 2a, main text), the voltage drop and electric field gradient in the top channel are likely similar to that observed in the bottom channel with the difference being that voltage drops from the reservoirs toward the channel center where the ion depletion zone and region of high resistivity forms.

### Movie Files

**Movie S-1** initially shows  $\text{Ru}(\text{bpy})_3^{2+}$  depleting toward the reservoirs in the bottom channel via EM with the application of 30.0 V to  $V_1$ . Then, because  $\text{Ru}(\text{bpy})_3^{2+}$  depletion could only be monitored in one half of the microchannel during a single experiment,  $\text{Ru}(\text{bpy})_3^{2+}$  was observed to deplete into reservoir  $V_3$  (Scheme 2a, main text). Each frame of the movie represents 10 s of operation with the movie played at 10 fps. The duration of this depletion experiment was 144 s after the application of 30.0 V to  $V_1$ , while  $V_2$ ,  $V_3$ , and  $V_4$  were grounded.

**Movie S-2** was recorded with a fluorescence microscope (Multizoom AZ100, Nikon, Japan) in a top-down configuration fitted with a CCD camera (QuantEM 512SC, Photometrics, Tucson, AZ). The top-down geometry was used to monitor tracer above the BPE. Movie S-2 shows  $\text{BODIPY}^{2-}$  enriching to the right of the split BPE anode in the bottom channel with PDF ( $\sim 15 \mu\text{m/s}$ ) moving from left to right. Then, PDF was adjusted ( $\sim 15 \mu\text{m/s}$ , from right to left) to cause the enriched  $\text{BODIPY}^{2-}$  band to relocate to the left of the BPE anode. Each frame of the movie represents 5 s of operation with the movie played at 5 fps. The duration of this enrichment movie was 54 s. During this experiment, 30.0 V was applied to  $V_1$ , while  $V_2$ ,  $V_3$ , and  $V_4$  were grounded.

### References

1. G. Ocvirk, M. Munroe, T. Tang, R. Oleschuk, K. Westra, D. J. Harrison, *Electrophoresis*, 2000, **21**, 107-115.
2. R. K. Perdue, D. R. Laws, D. Hlushkou, U. Tallarek, R. M. Crooks, *Anal. Chem.*, 2009, **81**, 10149-10155.
3. R. K. Anand, E. Sheridan, D. Hlushkou, U. Tallarek, R. M. Crooks, *Lab Chip*, 2011, **11**, 518-527.
4. E. Sheridan, D. Hlushkou, R. K. Anand, D. R. Laws, U. Tallarek, R. M. Crooks, *Anal. Chem.*, 2011, **83**, 6746-6753.